Biological Journal of the Linnean Society, 2020, **XX**, 1–13. With 5 figures.

Phylogenetics and population structure of the steppe species *Hycleus polymorphus* (Coleoptera: Meloidae: Mylabrini) reveal multiple refugia in Mediterranean mountain ranges

ALESSANDRA RICCIERI[1*], EMILIANO MANCINI[2], MATTIA IANNELLA[3], DANIELE SALVI[3,4], and MARCO A. BOLOGNA[1]

[1]*Department of Sciences, University "Roma Tre", Viale G. Marconi 446, 00146 Roma, Italy*
[2]*Department of Biology and Biotechnology "C. Darwin", "Sapienza" University of Rome, Viale dell'Università 32, 00186 Roma, Italy*
[3]*Department of Health, Life & Environmental Sciences, University of L'Aquila, Via Vetoio snc, 67100 L'Aquila-Coppito, Italy*
[4]*CIBIO-InBIO, Centro de Investigação em Biodiversidade e Recursos Genéticos, Universidade do Porto, Campus Agrário de Vairão, 4485–661 Vairão, Portugal*

Received 24 February 2020; revised 31 March 2020; accepted for publication 1 April 2020

Many continental species distributed in the Eurasian steppe occur as relict populations in the mountains of Western Europe. Their biogeographical responses to Quaternary climate changes have been poorly studied; however, they could have responded as cold-adapted species. We investigated the biogeographic history of a steppe beetle, *Hycleus polymorphus*, using mitochondrial and nuclear DNA sequences (*COI*, *CAD*, ITS2), and species distribution modelling (SDM) under present and past bioclimatic envelopes. We first performed a phylogenetic assessment to define species boundaries within the *H. polymorphus* species group. Specimens previously treated as *Hycleus humerosus* on morphological grounds are assigned to *H. polymorphus*, and those identified as *Hycleus zebraeus* assigned to *Hycleus atratus*. ITS2 data analyses revealed a strong phylogeographical structure of *H. polymorphus* populations, with four haplogroups corresponding to the (i) Italian Alps, (ii) French Alps and Pyrenees, (iii) South Balkan and Pontic mountains, and (iv) North Dinaric Alps. Based on these analyses and the SDM, we propose that during a glacial period, following the spread of steppic habitat, *H. polymorphus* underwent a range expansion from Asia to South-West Europe. Within the Mediterranean area, during the last interglacial the climatic suitability for the species was limited to mountains that acted as refugia and prompted allopatric divergence into four main lineages.

ADDITIONAL KEYWORDS: *CAD* – *COI* – cold-adapted species – continental elements – fragmented distribution – ITS2 – Mediterranean mountains – phylogeography – Pleistocene climate oscillations – Species Distribution Models.

INTRODUCTION

The current distribution of organisms and their genetic diversity has been largely shaped by Pliocene and Pleistocene climatic fluctuations, especially in the northern hemisphere (Taberlet *et al.*, 1998; Hewitt, 1999, 2000, 2004; Petit *et al.*, 2003). In the Palaearctic Region, two types of biota have been documented by various authors based on response to Pleistocene climate fluctuations (Hewitt, 1999; Schmitt, 2007, 2017; Stewart *et al.*, 2010): a warm-adapted biota, where species ranges underwent a contraction during cold periods and an expansion during interglacial phases, and a cold-adapted biota, which showed a reverse pattern [but see Bisconti *et al.* (2011); Salvi *et al.* (2014) and Senczuk *et al.* (2019) for notable exceptions]. Recently, phylogeographical studies also focused on a third type of biota, the so-called "continental elements", currently distributed in steppes and steppe-like environments in plains and mountain areas from

*Corresponding author. E-mail: alessandra.riccieri@uniroma3.it

Central Asia to Eastern-Central Europe (Schmitt, 2007, 2017; Stewart *et al.*, 2010; Kajtoch *et al.*, 2016). Among these continental elements, some species also occur as isolated populations in the mountain ranges of South-Western Europe, which are considered relicts of a continuous distribution that occurred during periods of more favourable climate [e.g. *Parnassius apollo* (Todisco *et al.*, 2010); *Vipera ursinii-renardi* complex (Ferchaud *et al.*, 2012)]. Previous studies suggested that continental species are likely to expand their range along a longitudinal axis (instead of latitudinal) from east to west during glacials and to retreat eastward during interglacials following steppe expansions and contractions (Schmitt, 2007, 2009, 2017; Stewart *et al.*, 2010). Consequently, they should display a longitudinal decrease of genetic diversity from east to west (Schmitt, 2007; Stewart *et al.*, 2010). However, the review by Kajtoch *et al.* (2016) pointed out that steppe species studied so far do not exhibit a generalized east-west expansion and contraction pattern, but rather show several separate interglacial refugia across their range as do cold-adapted species.

The blister beetle *H. polymorphus* (Pallas, 1771), is an example of a steppe species with a disjunct Central Asiatic–Western European distribution and represents an interesting opportunity to explore the biogeographic processes underlying this distribution pattern. *H. polymorphus* belongs to the largest genus of Meloidae and is part of a group of 14 species mainly centred in the steppes and grasslands of Western-Central Asia (Bologna, 1991; Pan *et al.*, 2017; Riccieri *et al.*, 2020). Based on the current distribution of this species group, we can assume an ancestral Asiatic origin for *H. polymorphus*. Within its group, *H. polymorphus* is the only species with a disjunct pattern with western populations isolated on Mediterranean mountain ranges (Bologna, 1991; Bologna & Pinto, 2002). Specifically, its current distribution is continuous from the steppes of Central Asia to Eastern Europe, usually at both middle- and high-altitudes, whereas in South-Western Europe it occurs as isolated populations associated with prairies and xeric pastures on the Pyrenees, the Alps and mountain ranges of the Balkan Peninsula [mostly between ~900 and ~2000 m a.s.l. (Bologna, 1991, 1994)].

This study focuses on the Mediterranean populations of *H. polymorphus*. We investigate the response of this steppe species to Pleistocene climate changes and the biogeographic processes underlying its current pattern of fragmented distribution. We first assess the *H. polymorphus* species group phylogenetically to better define species boundaries, since some species of the group are often confused morphologically [e.g. *H. zebraeus* (Marseul, 1870) with *H. polymorphus*; *Hycleus chodschenticus* (Ballion, 1878) with *Hycleus solonicus* (Pallas, 1782) (Bologna, 1991, 1994; Pan *et al.*, 2017)]. We then investigate the genetic structure and evolutionary history of *H. polymorphus* populations based on mitochondrial and nuclear DNA sequence data, together with species distribution modelling under present and past bioclimatic conditions. Our hypothesis is that the biogeographic history of *H. polymorphus* in the Mediterranean area reflects the cyclic expansion and contraction of steppe habitat in this region during the Pleistocene. Thus, its current fragmented distribution represents interglacial isolation in mountain refugia.

MATERIAL AND METHODS

Taxon sampling and dataset preparation

Samples used for this study were collected from 1999 to 2018 and were all stored in ethanol 96% at 4 °C, except one killed in ethyl-acetate and pinned. Specimen identification was based on the dichotomous keys published by Marseul (1870) and Sumakov (1915), and a taxonomic study by Bologna (1994).

Two different datasets were used: the first dataset, used for phylogenetic inference, included 53 morphologically identified specimens (Supporting Information, Table S1) belonging to different populations of the following taxa: *H. atratus* (Pallas, 1773) ($N = 5$), *Hycleus fuscus* (A.G. Olivier, 1811) ($N = 6$), *H. humerosus* (Escherich, 1899) ($N = 4$), *H. polymorphus* ($N = 18$), *Hycleus scabiosae* (A.G. Olivier, 1811) ($N = 7$), *H. solonicus* ($N = 2$), *Hycleus tekkensis* (Heyden, 1883) ($N = 1$), *H. zebraeus* ($N = 7$), *H.* cfr. *zebraeus* ($N = 2$), and *Mylabris sinuata* Klug, 1845 ($N = 1$) as the outgroup. The second dataset, used for phylogeographical analyses, included 90 specimens of *H. polymorphus* from 22 localities from the Mediterranean area (Fig. 1; Table 1 and Supporting Information, Table S2), plus four specimens of *H. humerosus*, which phylogenetic investigation nested within the *H. polymorphus* clade (see *Results*).

DNA extraction, gene amplification, sequencing and alignment

Following the salting out protocol (Sambrook *et al.*, 1989), total genomic DNA was extracted from one to three legs of each specimen, eluted in 100 µL of pure H_2O and stored at -20 °C. DNA extraction from the pinned sample utilized the procedure described by Gilbert *et al.* (2007) as modified by Giordani (2019).

Three genetic markers were amplified by PCR: the cytochrome oxidase subunit I (*COI*); the carbamoylphosphate synthetase domain of the rudimentary gene (*CAD*); and the internal transcribed spacer (ITS2). PCR amplifications were carried out in a total volume of 25 µL with 3 µL of 10x reaction

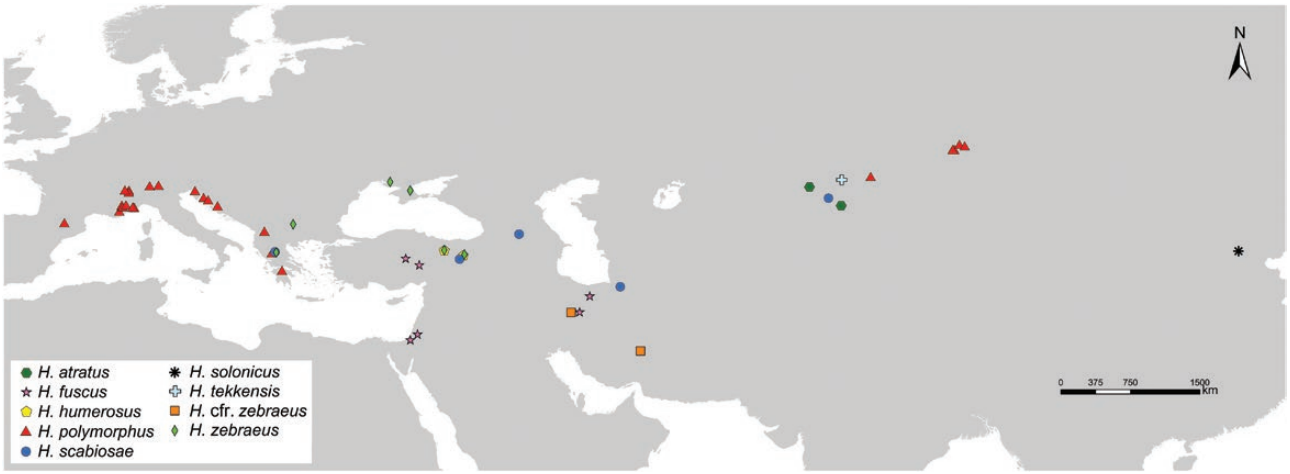

Figure 1. Geographical distribution of sampled localities of *H. atratus*, *H. fuscus*, *H. humerosus*, *H. polymorphus*, *H. scabiosae*, *H. solonicus*, *H. tekkensis*, *H.* cfr. *zebraeus* and *H. zebraeus*.

buffer, 1/1.5/2 µL of $MgCl_2$ (50mM), 0.5/1 µL dNTPs (10 mM), 0.2 µL of TaqDNA polymerase (5 U/µL; BIOTAQ Bioline), 0.5µL of each primer (25 mM) and 1 µL of DNA template. Primer pairs and thermal cycles followed Salvi *et al.* (2019) and Riccieri *et al.* (2017, 2020). Purification and sequencing of amplified products was provided by Macrogen. In addition, 15 sequences for *CAD* and 12 for *COI* were downloaded from GenBank (see Supporting Information, Tables S1-S2). Sequences were deposited in GenBank with the following accession numbers: CAD = MT263176 - MT263281; COI = MT261069 - MT261109; ITS2 = MT259464 (for further details see Supporting Information, Tables S1-S2).

Sequences were edited with the program Staden Package v.4.11.2 (Staden *et al.*, 2000), and aligned with MAFFT (Katoh *et al.*, 2019). Due to numerous indels in the ITS2 alignment including different species, ambiguous and poorly aligned positions were removed with the GBLOCKS server v.0.91b (Castresana, 2000).

Phylogenetic analysis of the species group

Phylogenetic analyses were performed on single genes and multilocus datasets using the web portal CIPRES (http://www.phylo.org). The best substitution model for each gene partition was selected with JModeltest v.2.1.6 (Posada, 2008) based on the Akaike Information Criterion (AIC). Maximum Likelihood (ML) analysis was carried out with RAxML-HPC v.8.2.10 (Stamatakis, 2006) with a partitioned GTRGAMMA model and a rapid-bootstrap analysis with 1000 replicates. Bayesian Inference (BI) utilized MrBayes v.3.2.6 (Ronquist *et al.*, 2012) with the following settings: two independent runs with four Markov chains each were run for 10 million generations sampling trees every 1000 generations with a 10% burn in. Tracer v.1.6 (Rambaut *et al.*, 2015) was used to confirm run convergence, and FigTree v.1.3.1 (Rambaut & Drummond, 2009) was used to visualize the tree.

Phylogeography of *H. polymorphus*

Some *COI* chromatograms showed a few double peaks, probably due to heteroplasmy. Therefore, we avoided using *COI* sequences in the phylogeographical analyses since the impact of these heterozygotic sites in the estimation of intraspecific relationships can be higher relative to interspecific comparisons.

Reconstruction of nuclear haplotypes utilized the PHASE algorithm implemented in DNAsp v.6 (Rozas *et al.*, 2017). Relationships among haplotypes were inferred using both the Median Joining algorithm (Bandelt *et al.*, 1999) implemented in NETWORK v.4.6 (http://www.fluxus-engineering.com), and the statistical parsimony network approach implemented in the software TCS v.1.21 (Clement *et al.*, 2000) with gaps treated as 5th state characters. TcsBU (Santos *et al.*, 2015) was used to draw the networks. For downstream analyses, sequences were grouped according to the ITS2 haplogroups. Specimens not amplified for ITS2 were excluded from the *CAD* dataset. Number of segregating sites (S) and haplotypes (H), haplotype diversity (Hd) and nucleotide diversity (π) were computed with DNAsp v.6 (Rozas *et al.*, 2017) for the entire dataset and for each haplogroup (Table 1). Arlequin v.3.5 (Excoffier & Lischer, 2010) was used to estimate F_{st} values between haplogroups, based on *CAD*, and to perform analysis of molecular variance (AMOVA) (Excoffier *et al.*, 1992) based on ITS2, in order to assess genetic differentiation within populations, among populations within groups and among groups.

Table 1. Sampled localities and relative altitude, coordinates, collection date and number of individuals analysed for each marker

Species	LOCALITIES			ALTITUDE (m a.s.l.)	COORDINATES	DATES (dd/mm/yy)	*CAD*	ITS2
H. humerosus	Turkey	T1	Sivas	1720	39°57'29.88"N, 37°56'33.04"E	03/07/2010	1	1
		T2	Tunceli	1680–1850	39°27'10.71"N, 39°46'40.06"E	22/06/2013	3	2
H. polymorphus	Croatia	C1	Krk Island	350	45°01'25.48"N, 14°20'26"E	21/05/2017	1	1
		C2	Krasno Polje	1020	44°51'43"N, 14°53'33"E	18/07/2017	1	1
		C3	Vučipolje	832	44°15'17"N, 15°56'59"E	15/06/2018	5	5
	Albania	A1	Korab Mts.	1700	41°48'07"N, 20°29'56"E	21/07/2017	4	4
	Greece	G1	Ioannina, Metsovo, Peristéri Mts	1750	39°42'18.90"N, 21°12'37.83"E	06/07/2009	5	5
		G2	Kalavrita, Aroania Mts	1610	38°00'27.03"N, 22°11'56.61"E	08/07/2009	5	5
	Italy	I1	Liguria, Col di Nava (IM)	850	44°06'17.44"N, 07°52'13.86"E	23/6/2017	9	7
		I2	Piemonte, Carnino (CN)	1700	44°08'52.20"N, 07°44'6.79"E	27/07/2018	1	1
		I3	Piemonte, Upega (CN)	1350	44°07'56"N, 07°42'54"E	24/06/2017	2	0
		I4	Piemonte, Sambuco (CN)	1300–1500	44°20'39.4"N, 07°04'15.5"E	29/06/2011	7	6
		I5	Valle d'Aosta, Valnontey (AO)	1899	45°35'8.48"N, 07°19'56.42"E	10/07/2010	10	8
		I6	Valle d'Aosta, Chécrouit (AO)	2200	45°47'22.83"N, 06°57'41.80"E	07/08/2018	4	3
		I7	Valle d'Aosta, Blavy (AO)	1460	45°46'28"N, 07°20'28"E	15/07/2017	5	5
		I8	Lombardia, Montemezzo (CO)	1050	46°12'16.74"N, 09°21'39.67"E	14/07/2017	5	4
		I9	Lombardia, Vervio (SO)	1430–1520	46°15'26"N, 10°13'10"E	16/07/2017	5	4
		I10	Friuli Venezia Giulia, Sgonico (TS)	270–300	45°43'59"N, 13°45'15"E	03/06/2012	3	1
	France	F1	Var, Trigance	995	43°44'57"N, 06°24'56"E	25/06/2017	5	5
		F2	Alpes d'Haute Provence, Villard d'Abbas	1535	44°19'22"N, 06°39'45"E	29/06/2017	3	3
		F3	Alpes Maritimes, Entraunes	1200	44°10'25"N, 06°44'60"E	29/06/2017	5	5
	Spain	S1	Lerida, Valencia de Aneu	1700	42°37'21.72"N, 01°4'54.68"E	n.a.*	0	1
	Total populations		22		Total		89	77

* n.a. = Not available. In brackets Italian provinces abbreviations: IM = Imperia, CN = Cuneo, AO = Aosta, CO = Como, SO = Sondrio, TS = Trieste.

Species distribution model building and evaluation

To infer current and past climatic suitability for the target species, nineteen bioclimatic variables from Worldclim.org were downloaded at 2.5 arc-min resolution (v.1.4) (Hijmans *et al.*, 2005). For past climatic scenarios, we used the Last Inter-Glacial [LIG, about 120 000–140 000 years ago, from Otto-Bliesner *et al.* (2006)] and Last Glacial Maximum (LGM, about 22 000 years ago) variables. For the LGM, to account for differences among Global Climate Models [GCMs (Zhang *et al.*, 2015; Ashraf *et al.*, 2017; Cerasoli *et al.*, 2019)], we used all the three available GCMs: the CCSM4 (Gent *et al.*, 2011), the MIROC-ESM (Watanabe *et al.*, 2011) and the MPI-ESM-P (Jungclaus *et al.*, 2013). Multicollinearity among predictors was assessed by calculating a correlation matrix in ArcMap v.10.0 (ESRI, 2010). We retained only variables that were not strongly correlated with each other [Pearson's correlation coefficient, $|r| > 0.80$ (Dormann *et al.*, 2013)] and that we deemed as more biologically significant for *H. polymorphus* (Brandt *et al.*, 2017; D'Alessandro *et al.*, 2018; Brunetti *et al.*, 2019).

To account for spatial correlation among the localities of *H. polymorphus*, the initial dataset of 576 occurrences was rarefied through the 'spThin' package (Aiello-Lammens *et al.*, 2015), with a minimum locality distance set to 5 km in R (R Core Team, 2016). A Moran test was further performed in ArcMap v.10.0 (ESRI, 2010) to check correlation among records of the rarefied dataset.

Species Distribution Models (SDMs) for the target species utilized the 'biomod2' package (Thuiller *et al.*, 2016) in R (R Core Team, 2016). The algorithms within this package allow the creation of the so-called "Ensemble Models" (EMs), models resulting from the proportional combination of responses from single modelling techniques, taking advantage of the pros and minimizing the cons of each (Araújo & New, 2007; Thuiller *et al.*, 2009; Thuiller *et al.*, 2016). The algorithms used to calibrate our models were Generalized Linear Models (GLMs, type = 'quadratic', interaction level = 3), Multiple Adaptive Regression Splines (MARS, type = 'quadratic', interaction level = 3) and Gradient Boosting Models (GBM, sometimes known as BRTs; number of trees = 10 000, interaction depth = 3 and 10-fold cross validation), in order to encompass and merge different statistical approaches. Ten sets of 1000 pseudo-absences each were generated within an area corresponding to the 95th quantile of a linear model built over the presence data ('surface range envelope' algorithm) (Chefaoui & Lobo, 2008). The 'BIOMOD_Modelling' function was used to calibrate models.

Of the starting dataset, 20% was used for model testing and 80% for calibration. Five evaluation runs were performed, obtaining a total of 150 single models, whose performances were assessed through the Area Under the Curve (AUC) of the Receiver Operator Characteristics (ROC) (Phillips *et al.*, 2006) and the True Skill Statistic (TSS) (Allouche *et al.*, 2006). Only models having both AUC > 0.8 and TSS > 0.7 were selected for the Ensemble Modelling process (see Iannella *et al.*, 2018). The 'wmean' algorithm (weighted mean of probabilities) of the 'BIOMOD_EnsembleModeling' function was used to build the Ensemble Model. This is a procedure which proportionally assigns a score when building the ensemble based on each model performance. The 'BIOMOD_EnsembleForecasting' function was used to project the calibrated model to the past climatic scenarios.

Considering that multiple projections to novel environments (i.e. different and very long time frames) were performed and had to be combined (the three different GCMs for the LGM scenario), possible extrapolation was assessed and corrected through the Multivariate Environmental Similarity Surface [MESS (Elith *et al.*, 2010)] and the Multivariate Environmental Dissimilarity Index [MEDI (Iannella *et al.*, 2017)] algorithms, respectively. Extrapolation may occur when dealing with projections in space and time because of possible differences (in terms of values) between the projected scenario's variables and the ones used for model calibration. To assess these differences, the 'mess' function of the 'dismo' R package (Hijmans & Elith, 2016) was applied to each past projection, obtaining a map for each; these maps were further processed in ArcMap v.10.0 (ESRI, 2010) applying the MEDI algorithm, a procedure which takes extrapolation into account and proportionally down-weighs models when performing an average model (Iannella *et al.*, 2017).

RESULTS

Phylogeny of the *H. polymorphus* species group

Our final dataset consisted of 1731 bp (*CAD*: 782 bp, 50 sequences; *COI*: 577 bp, 53 sequences; ITS2: 372 bp, 40 sequences).

Overall, ML and BI results were consistent among multilocus (Fig. 2) and single-gene datasets (Supporting Information, Fig. S1). In almost all resulting trees, samples were grouped in well-supported clades; however, deeper relationships received lower support. In particular, seven clades were recovered in the multilocus BI tree (Fig. 2A) corresponding to each nominal species, with two exceptions: specimens of *H. zebraeus* were included in the clade of *H. atratus*

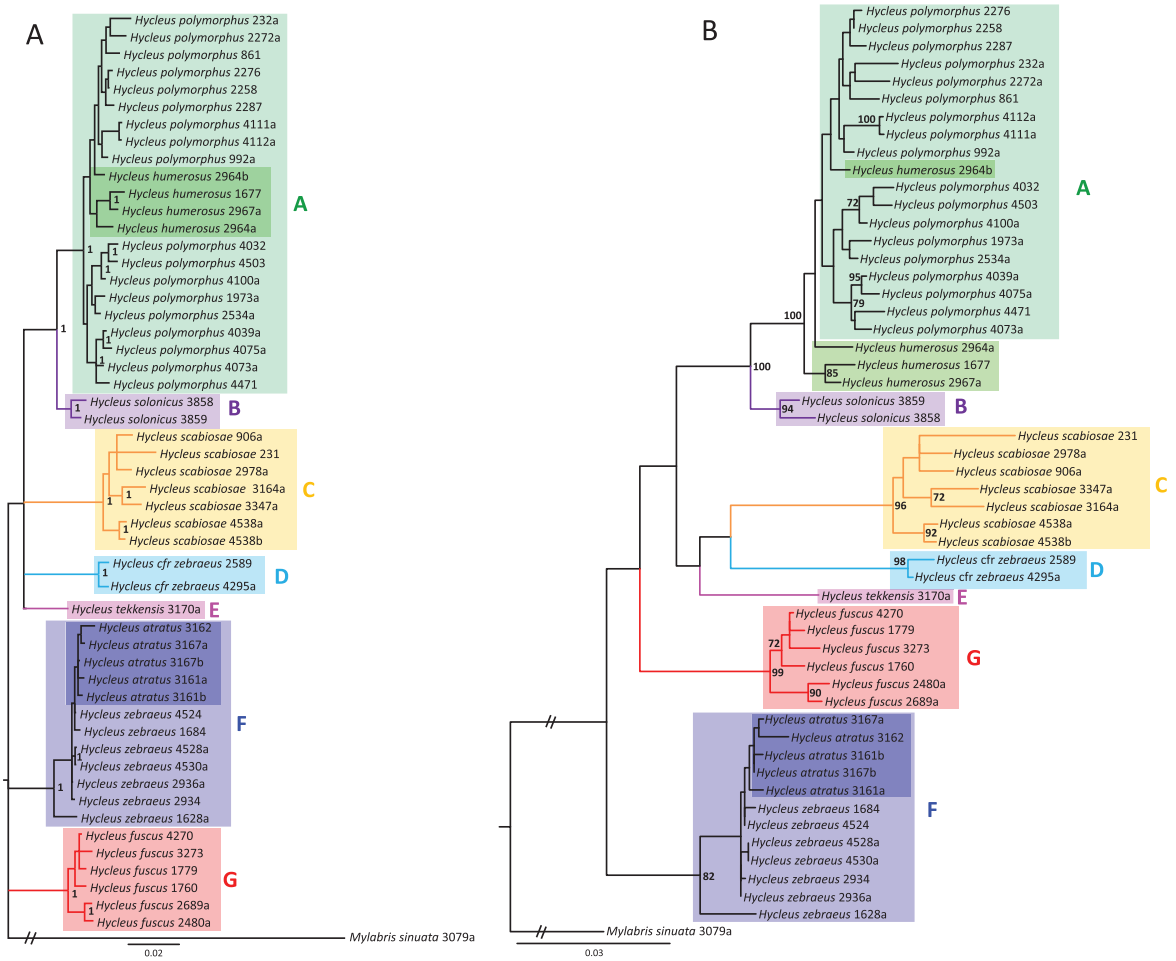

Figure 2. (A) BI and (B) ML multilocus (*CAD*, *COI*, ITS2) trees. Different colours are assigned to species clades. Supported values of Bayesian Posterior Probability (PP > 0.9) and Bootstrap (BS > 70) are reported at nodes.

(clade F), and those of *H. humerosus* were nested within the clade of *H. polymorphus* (clade A). In the multilocus ML tree (Fig. 2B), as well as in the *COI* ML tree (Supporting Information, Fig. S1), two of four samples of *H. humerosus* formed a sister group of a clade including all *H. polymorphus* and the remaining *H. humerosus*. Only in the phylogenetic trees based on the ITS2 were *H. solonicus* and *H. polymorphus* intermixed in the same clade (Supporting Information, Fig. S1).

PHYLOGEOGRAPHY OF *H. POLYMORPHUS*

The phylogeographical dataset of *H. polymorphus* consisted of 154 (phased) sequences of ITS2 (376 bp) and 178 (phased) sequences of *CAD* (748 bp). Overall *CAD* resulted in considerable polymorphism (165 haplotypes; Table 2) with 152 heterozygous positions (20.3%), two-thirds of them (66%) in third position, whereas ITS2 showed less polymorphism (17 haplotypes; Table 2) and fewer heterozygous positions (2.5%).

The median joining algorithm and the statistical parsimony network approach gave identical results, so we report only the haplotype networks obtained with TCS v.1.21 (Clement *et al.*, 2000). The ITS2 haplotype network showed four main haplogroups (Fig. 4): (i) haplogroup 1 (H1) includes haplotypes from Italian Alpine populations; (ii) haplogroup 2 (H2) includes two haplotypes shared among populations from the Western Alps (France and one sample from South-West Italian Alps) and the Pyrenees (Spain); (iii) haplogroup 3 (H3) includes haplotypes from the Southern Balkan mountains (Greece and Albania) and the North-Eastern Pontic mountains (Turkey); (iv) haplogroup 4 (H4) includes haplotypes from the Dinaric Alps (Croatia). H1 represents the core of the network, i.e. it is connected with all the other haplogroups that have a terminal position and are separated from H1 respectively by: H2 = 6 mutational steps; H3 = 7

Table 2. DNA polymorphism of *CAD* and ITS2. Sequences were grouped according to haplogroups observed in the ITS2 network

	Haplogroups	2n	S	*H*	*Hd* (%)	π (%)
CAD (748 bp)	Overall	178	159	165	99.9	2.3
	H1	76	97	69	99.7	2.0
	H2	28	56	26	99.5	1.8
	H3	34	74	33	99.8	2.1
	H4	14	58	14	1.0	2.4
ITS2 (376 bp)	Overall	154	27	17	90.0	2.0
	H1	76	4	7	77.1	0.4
	H2	30	1	2	51.5	0.1
	H3	34	3	5	48.0	0.2
	H4	14	2	3	71.4	0.2

n = Number of alleles.

S = Number of segregating sites.

H = Number of haplotypes.

Hd = Haplotype diversity.

π = Nucleotide diversity.

mutational steps; H4 = 9 mutational steps. Within the ITS2 alignment some haplogroup-specific signature sequences [i.e. indel shared among specific OTUs (see Trizzino *et al.*, 2009)] were detected (Fig. 3). AMOVA results supported this strong subdivision with 89% of genetic variance distributed among groups ($P < 0.05$).

The haplotype network of *CAD* did not show any phylogeographical structure (i.e. no clear haplotype/haplogroup segregation) although *CAD* F_{st} values scored between haplogroup pairs were all statistically supported ($P > 0.005$) and ranged between 0.10–0.20, with the highest value observed between H2 and H3.

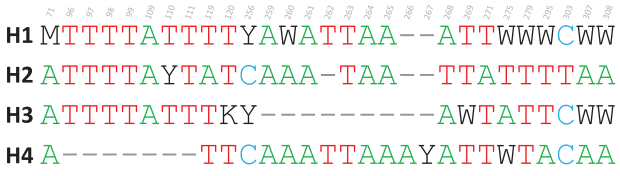

Figure 3. Partial ITS2 alignment showing variable positions and signature sequences (i.e. indels). On the left, for each sequence is indicated the corresponding haplogroup highlighted in the haplotype network.

Distribution models

The bioclimatic predictors selected for the modelling process were BIO2 (mean diurnal range), BIO6 (minimum temperature of the coldest month), BIO7 (temperature annual range), BIO10 (mean temperature of the warmest quarter), BIO11 (mean temperature of the coldest quarter) and BIO18 (precipitation of the warmest quarter). After the thinning process, 343 localities were chosen for model building and calibration. These showed no spatial correlation, with Moran's I = -0.0008 (expected value = -0.0004), z-score = -0.849 and P = 0.395. The EMs obtained through the 'wmean' algorithm reported high values of AUC (= 0.987) and TSS (= 0.887). BIO6, BIO10 and BIO11 were the three most contributing variables, with 44.8%, 20.7% and 9.3% of the total contribution, respectively. The suitability maps obtained for the current scenario showed high conformity between the predicted suitable areas and the occurrence localities, with the Pyrenees, Alps and part of the Balkan mountain areas having the highest suitability values (Fig. 5C). For past projections, the LGM scenario (Fig. 5B) showed a south-western shift, with a general increase of areas with high and very high climatic suitability. Climatic suitability during the LIG was confined to mountain territories (Fig. 5A), similar to the current asset.

DISCUSSION

Palaearctic steppes, among the largest continuous biomes on earth, have existed as a wide belt connecting Asia and Europe. This habitat underwent expansions and contractions throughout the ice ages (Kajtoch *et al.*, 2016; Wesche *et al.*, 2016, Bartonova *et al.*, 2018). Particularly during European interglacial phases, steppe environments were likely confined to eastern and south-eastern regions, repeatedly spreading westward during colder and dryer glacial phases (Kajtoch *et al.*, 2016). Following this pattern, steppe species underwent severe range shifts

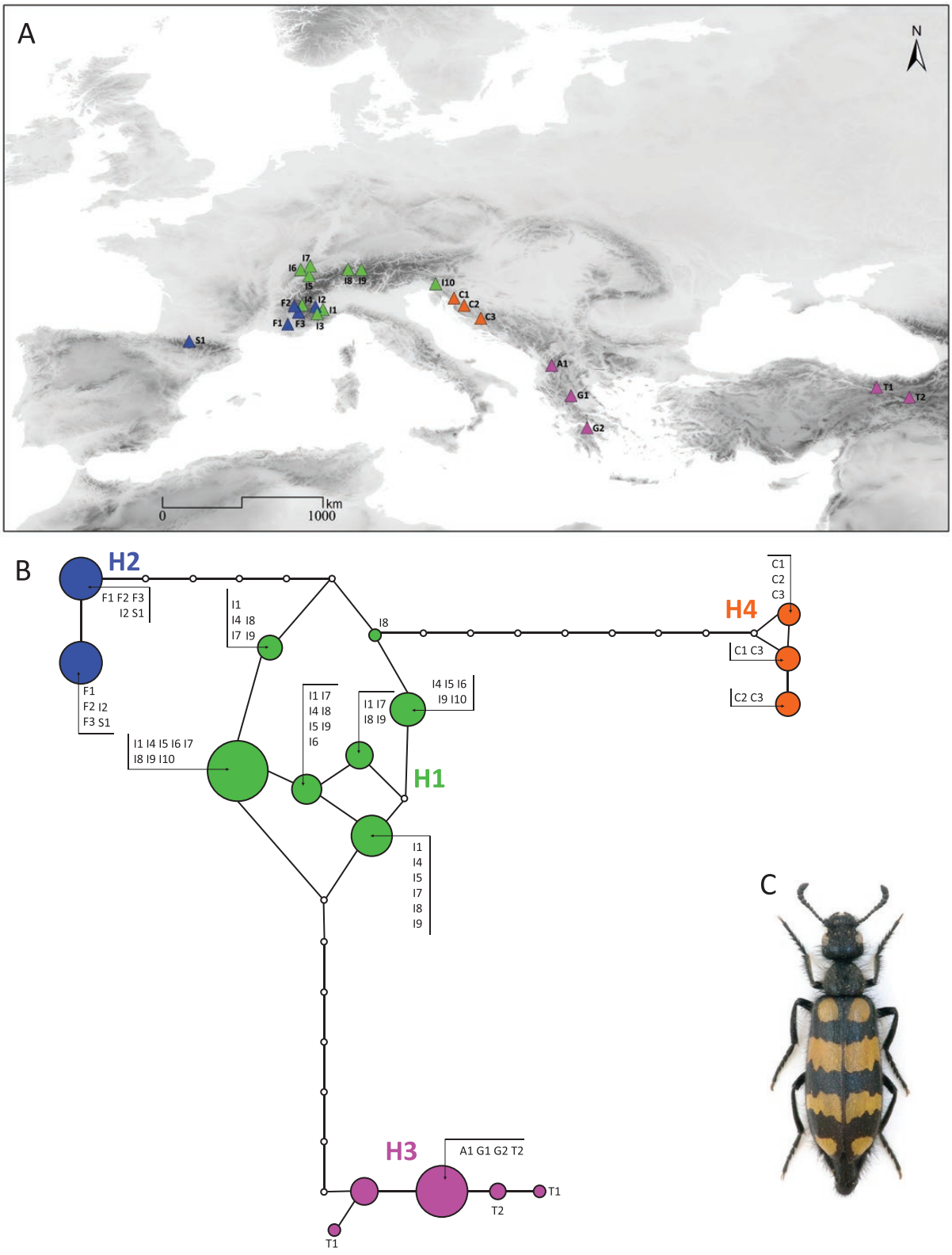

Figure 4. (A) map showing the geographic distribution of the main haplogroups. (B) haplotype parsimony network of ITS2. Haplotypes are represented by circles with size proportional to their frequency. The geographic origin of the samples included in each haplotype is indicated with the codes reported in Table 1. C, *H. polymorphus*.

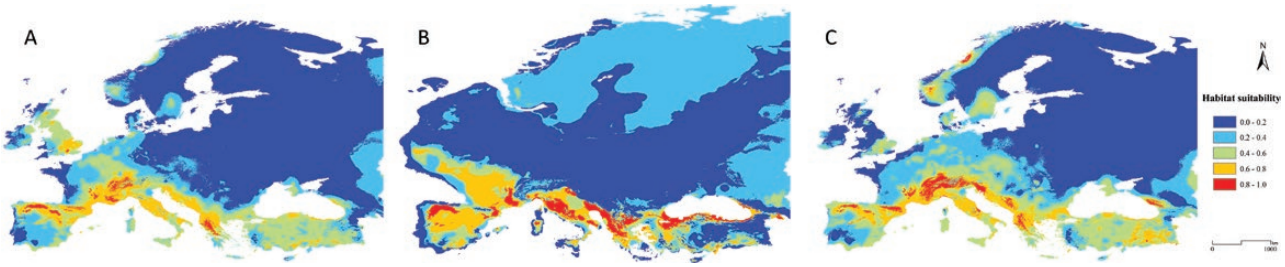

Figure 5. Habitat suitability (inferred from bioclimatic variables) obtained for *H. polymorphus* for (A) the last interglacial stage, LIG (~120 000–140 000 years ago), (B) the last glacial maximum, LGM (~22 000 years ago) and (C) current climatic conditions.

and fragmentations during Pleistocene climatic fluctuations which affected the genetic structure of their populations (Kajtoch *et al.*, 2016).

The evolutionary and biogeographic history of the steppe beetle *H. polymorphus* conforms to a pattern of interglacial contraction and glacial expansion; however, it also suggests a long-term persistence of populations in its western range during interglacial phases.

Phylogeographical analyses revealed a strong population structure of *H. polymorphus* in the Mediterranean region with four main lineages distributed in distinct mountain ranges: an Italian lineage (H1), a Western lineage (H2), an Eastern lineage (H3) and a Dinaric lineage (H4) (Fig. 4). This genetic structure suggests a scenario of allopatric divergence in distinct mountain refugia within the Mediterranean area. Based on the distribution of climatic suitability for this species during the last glacial and interglacial phases as inferred from SDMs, it is likely that these areas represented interglacial refugia (Fig. 5). Indeed, while suitable bioclimatic conditions were widespread across the Mediterranean region during the LGM (Fig. 5B), during the LIG highly suitable areas appeared to be more fragmented and restricted to mountain ranges, including the Pyrenees, French, Italian and Dinaric Alps, and Southern Balkan mountains (Fig. 5A). In absence of a molecular divergence rate for the markers used, an estimate of divergence time between lineages is not possible with our data. However, a recent (Late Pleistocene) divergence underlying the population structure observed in *H. polymorphus* might be supported by the lack of lineage sorting observed at the *CAD* locus. Indeed, this marker showed complete lineage sorting for older (Pliocene) divergence events as observed in the blister beetles *Mylabris schreibersi* Reiche, 1866 and *Cabalia segetum* (Fabricius, 1792) (Riccieri *et al.*, 2017).

Whereas the Italian (H1) and Dinaric lineages (H4) are continuously distributed, the Western (H2) and Eastern lineages (H3) are disjunct (Fig. 4). The Western lineage occurs in the Pyrenees and French Alps, where it overlaps the Italian lineage (H1). This overlap was possibly due to secondary contact between both lineages established during a favourable glacial stage (see Fig. 5B; Schmitt, 2009, 2017). Therefore, it appears that the range of the Western lineage was continuous during glacial periods and the current fragmented distribution is relictual. The same hypothesis can explain the disjunct distribution of the Eastern lineage (H3) in the Southern Balkan and Pontic mountains. In this regard we note that specimens from Turkey (Fig. 4) morphologically assigned to *H. humerosus* are treated as *H. polymorphus* in our phylogenetic analyses (Fig. 2A-B). This suggested synonymy needs to be considered once a larger sample is analysed [the same applies to *H. atratus* and *H. zebraeus* (Fig. 2A-B)].

Populations from the Dinaric Alps (C1-3: lineage H4; Fig. 4) belong to a lineage distinct from Southern Balkan populations (A1, G1, G2; lineage H3; Fig. 4). The clear distinction between North and South Balkans lineages also observed in the steppe butterfly *Proterebia afra* (Fabricius, 1787), was explained by climatic differences in the two areas during the LGM (Bartonova *et al.*, 2018). Interestingly, no genetic affinities were observed between populations from the Dinaric Alps (C1-3, H4; Fig. 4) and a nearby population from the Karst region (I10; Fig. 4). Instead, the latter is closely related to all other Italian Alpine populations (H1; Fig.4). This pattern is contrary to studies of many other groups of animals and plants which show the Karst having clearly greater biogeographic affinities with Dinaric and Illyric areas than with the Alpine zone [e.g. insects (Bologna, 1991); vertebrates (Bologna & Balletto, 2007); plants (Poldini, 2009)].

In conclusion, the observed population structure of *H. polymorphus* in the Mediterranean region suggests that this species acted as a cold-adapted species (Kajtoch *et al.*, 2016) in response to Pleistocene climate oscillations. According to our hypothesis, *H. polymorphus* expanded its range during glacial phases from Central Asia to South–Western Europe, following the spread of steppe environments, whereas during interglacial phases, populations in

the Mediterranean area were confined to higher altitudes in various mountain ranges. A similar scenario was hypothesized for the meadow viper *Vipera ursinii* (Bonaparte, 1835), whose current populations in mountain ranges are considered 'relictual' (Ferchaud *et al.*, 2012). In fact, in this species a significant decrease of habitat suitability in Western European mountains during interglacial periods was likely associated with the upward shift of the tree line and consequent decrease of grassland environments at lower altitudes (Ferchaud *et al.*, 2012). Despite the fact that the pattern observed in *H. polymorphus* matches that recorded so far for other steppe species confined to Mediterranean mountains, additional phylogeographical studies on "continental elements" are required before drawing general conclusions on the effect of biogeographical history on the peculiar distribution and population structure of these faunal elements.

ACKNOWLEDGMENTS

We would like to thank people who provided samples for this study, or helped us in field collection: P. Audisio (Roma, Italy), G. Belmonte (Lecce, Italy), M. Bologna (Roma, Italy), W. Beier (Germany), F. Cerini (Roma, Italy), P. Cerretti (Roma, Italy), L. Čížek (Ceske Budejovice, Czech Rep.), G. Cristiani (Alassio, SV, Italy), S.H. Dong (Hebei, China), L. Fekrat (Mashhad, Iran), G. Gardini (Genova, Italy), C. Giusto (Genova, Italy), S. Kolov (Alma Ata, Kazakhstan), S.S. Liu (Hebei, China), G. Mariani (Italy), Z. Pan (Hebei, China), R. Poloni (Modena, Italy), R. Poggi (Genova, Italy), P. Rapuzzi (Cialla di Prepotto, UD, Italy), R. Sindaco (Torino, Italy), the late A. Vigna Taglianti (Roma, Italy), V. Volpe (Roma, Italy), M. Zapparoli (Viterbo, Italy), S. Zoia (Milano, Italy). We thank two referees for their useful comments and John D. Pinto, Professor Emeritus of the University of California, Riverside, for improving the English. This study was supported by a PhD scholarship to A.R. and by grants to M.A.B. from MIUR, Ministero dell'Istruzione, dell'Università e della Ricerca, Italy (Programmi di ricerca scientifica di rilevante interesse nazionale: PRIN 99C5271884-007; PRIN 2004057217 "Zoogeography of Mediterranean-southern African disjunct distributions by a multimethod approach'; CRUI "Programma di mobilità Pietro della Valle" 2017), and from the University Roma Tre, Department of Science (grants of Departments of Excellence - L. 232/2016 - art.1, commi 314–337 awarded to Dept. of Science - University Roma Tre - Rome - Italy for 2018–2022). D.S. is currently supported by the program 'Rita Levi Montalcini' (MIUR) for the recruitment of young researchers at the University of L'Aquila.

REFERENCES

Aiello-Lammens ME, **Boria RA**, **Radosavljevic A**, **Vilela B**, **Anderson RP. 2015.** spThin: an R package for spatial thinning of species occurrence records for use in ecological niche models. *Ecography* **38:** 541–545.

Allouche O, **Tsoar A**, **Kadmon R. 2006.** Assessing the accuracy of species distribution models: prevalence, kappa and the true skill statistic (TSS). *Journal of Applied Ecology* **43:** 1223–1232.

Araújo MB, **New M. 2007.** Ensemble forecasting of species distributions. *Trends in Ecology & Evolution* **22:** 42–47.

Ashraf U, **Peterson AT**, **Chaudhry MN**, **Ashraf I**, **Saqib Z**, **Rashid Ahmad S**, **Ali H. 2017.** Ecological niche model comparison under different climate scenarios: a case study of *Olea* spp. in Asia. *Ecosphere* **8:** e01825.

Bandelt HL, **Forster P**, **Röhl A. 1999.** Median-Joining networks for inferring intraspecific phylogenies. *Molecular Biology and Evolution* **16:** 37–48.

Bartonova A, **Konvicka M**, **Korb S**, **Kramp K**, **Schmitt T**, **Faltynek Fric Z. 2018.** Range dynamics of Palaearctic steppe species under glacial cycles: the phylogeography of *Proterebia afra* (Lepidoptera: Nymphalidae: Satyrinae). *Biological Journal of the Linnean Society* **125:** 867–884.

Bisconti R, **Canestrelli D**, **Colangelo P**, **Nascetti G. 2011.** Multiple lines of evidence for demographic and range expansion of a temperate species (*Hyla sarda*) during the last glaciation. *Molecular Ecology* **20:** 5313–5327.

Bologna MA. 1991. *Coleoptera Meloidae. Fauna d'Italia. XXVIII*. Bologna: Calderini.

Bologna MA, **1994.** I Meloidae della Grecia (Coleoptera). *Fragmenta Entomologica* **25:** 1–119.

Bologna MA, **Balletto E**, **2007.** Biogeografia. In: Lanza B, Andreone F, Bologna MA, Corti C, Razzetti E. eds. *Amphibia. Fauna d'Italia. XLII*. Bologna: Calderini, 47–56.

Bologna MA, **Pinto JD. 2002.** The Old World genera of Meloidae (Coleoptera): a key and synopsis. *Journal of Natural History* **36:** 2013–2102.

Brandt LA, **Benscoter AM**, **Harvey R**, **Speroterra C**, **Bucklin D**, **Romañach SS**, **Watling JI**, **Mazzotti FJ. 2017.** Comparison of climate envelope models developed using expert-selected variables versus statistical selection. *Ecological Modelling* **345:** 10–20.

Brunetti M, **Magoga G**, **Iannella M**, **Biondi M**, **Montagna M. 2019.** Phylogeography and species distribution modelling of *Cryptocephalus barii* (Coleoptera: Chrysomelidae): is this alpine endemic species close to extinction? *ZooKeys* **856:** 3–25.

Castresana J. 2000. Selection of conserved blocks from multiple alignments for their use in phylogenetic analysis. *Molecular Biology and Evolution* **17:** 540–552.

Cerasoli F, **Iannella M**, **Biondi M. 2019**. Between the hammer and the anvil: how the combined effect of global warming and the non-native common slider could threaten the European pond turtle. *Management of Biological Invasions* **10:** 428–448.

Chefaoui RM, **Lobo JM. 2008.** Assessing the effects of pseudo-absences on predictive distribution model performance. *Ecological Modelling* **210:** 478–486.

Clement M, **Posada D**, **Crandall KA. 2000.** TCS: a computer program to estimate gene genealogies. *Molecular Ecology* **9:** 1657–1659.

D'Alessandro P, **Iannella M**, **Frasca R**, **Biondi M. 2018.** Distribution patterns and habitat preference for the genera-group *Blepharida* s.l. in Sub-Saharan Africa (Coleoptera: Chrysomelidae: Galerucinae: Alticini). *Zoologischer Anzeiger* **277:** 23–32.

Dormann CF, **Elith J**, **Bacher S**, **Buchmann C**, **Carl G**, **Carré G**, **Marquéz JRG**, **Gruber B**, **Lafourcade B**, **Leitão PJ. 2013.** Collinearity: a review of methods to deal with it and a simulation study evaluating their performance. *Ecography* **36:** 27–46.

Elith J, **Kearney M**, **Phillips S. 2010.** The art of modelling range-shifting species. *Methods in Ecology and Evolution* **1:** 330–342.

ESRI. **2010.** *ArcMap 10.0*. Redlands: ESRI.

Excoffier L, **Lischer HE. 2010.** Arlequin suite ver 3.5: a new series of programs to perform population genetics analyses under Linux and Windows. *Molecular Ecology Resources* **10:** 564–567.

Excoffier L, **Smouse PE**, **Quattro JM. 1992.** Analysis of molecular variance inferred from metric distances among DNA haplotypes: application to human mitochondrial DNA restriction data. *Genetics* **131:** 479–491.

Ferchaud AL, **Ursenbacher S**, **Cheylan M**, **Luiselli L**, **Jelić D**, **Halpern B**, **Major A**, **Kotenko T**, **Keyan N**, **Crnobrnja-Isailović J**, **Tomović L**, **Ghira I**, **Ioannidis Y**, **Arnal V**, **Montgerald C. 2012.** Phylogeography of the *Vipera ursinii* complex (Viperidae): mitochondrial markers reveal an east–west disjunction in the Palaearctic region. *Journal of Biogeography* **39:** 1836–1847.

Gent PR, **Danabasoglu G**, **Donner LJ**, **Holland MM**, **Hunke EC**, **Jayne SR**, **Lawrence DM**, **Neale RB**, **Rasch PJ**, **Vertenstein M. 2011.** The community climate system model version 4. *Journal of Climate* **24:** 4973–4991.

Gilbert MT, **Moore W**, **Melchior L**, **Worobey M. 2007.** DNA extraction from dry museum beetles without conferring external morphological damage. *PloS One* **2:** e272.

Giordani G. 2019. *Non-invasive approaches to morphological and molecular identification of insects from museum, archaeo-funerary and forensic contexts.* Unpublished D. Phil. Thesis, University of Huddersfield.

Hewitt GM. 1999. Post-glacial re-colonization of European biota. *Biological Journal of the Linnean Society* **68:** 87–112.

Hewitt GM. 2000. The genetic legacy of the Quaternary ice ages. *Nature* **405:** 907–913.

Hewitt GM. 2004. Genetic consequences of climatic oscillation in the Quaternary. *Philosophical Transactions of the Royal Society of London B* **359:** 183–195.

Hijmans RJ, **Cameron SE**, **Parra JL**, **Jones PG**, **Jarvis A. 2005.** Very high resolution interpolated climate surfaces for global land areas. *International Journal of Climatology* **25:** 1965–1978.

Hijmans RJ, **Elith J. 2016.** *dismo-package: species distribution modeling with R. R package version 1.1-1*. Available at: http://cran.r-project.org/web/packages/dismo/index.html (date last accessed 19 May 2019).

Iannella M, **Cerasoli F**, **Biondi M. 2017.** Unraveling climate influences on the distribution of the parapatric newts *Lissotriton vulgaris meridionalis* and *L. italicus*. *Frontiers in Zoology* **14:** 55.

Iannella M, **D'Alessandro P**, **Biondi M. 2018.** Evidences for a shared history for spectacled salamanders, haplotypes and climate. *Scientific Reports* **8:** 16507.

Jungclaus J, **Fischer N**, **Haak H**, **Lohmann K**, **Marotzke J**, **Matei D**, **Mikolajewicz U**, **Notz D**, **Von Storch J. 2013.** Characteristics of the ocean simulations in the Max Planck Institute Ocean Model (MPIOM) the ocean component of the MPI-Earth system model. *Journal of Advances in Modeling Earth Systems* **5:** 422–446.

Kajtoch Ł, **Cieślak E**, **Varga Z**, **Paul W**, **Mazur MA**, **Sramkó G**, **Kubisz D. 2016.** Phylogeographical patterns of steppe species in Eastern Central Europe: a review and the implications for conservation. *Biodiversity and Conservation* **25:** 2309–2339.

Katoh K, **Rozewicki J**, **Yamada KD. 2019.** MAFFT online service: multiple sequence alignment, interactive sequence choice and visualization. *Briefings in Bioinformatics* **20:** 1160–1166.

Marseul SA de. 1870. Monographie des Mylabrides d'Europe, et des contrées limitrophes en Afrique et en Asie. *L'Abeille* **7:** 1–204.

Otto-Bliesner BL, **Marshall SJ**, **Overpeck JT**, **Miller GH**, **Hu A. 2006.** Simulating Arctic climate warmth and icefield retreat in the last interglaciation. *Science* **311:** 1751–1753.

Pan Z, **Bai QQ**, **Wang J**, **Ren GD. 2017.** Revision of *Hycleus solonicus* (Pallas, 1782) (Coleoptera: Meloidae, Mylabrini), with larval description and DNA barcoding. *Entomologica Fennica* **28:** 219–232.

Petit R, **Aguinagalde I**, **de Beaulieu JL**, **Bittkau C**, **Brewer S**, **Cheddadi R**, **Ennos R**, **Fineschi S**, **Grivet D**, **Lascoux M**, **Mohnty A**, **Müller-Starck G**, **Demesure-Musch B**, **Palmé A**, **Pedro Martin J**, **Rendell S**, **Vendramin GG. 2003.** Glacial refugia: hotspots but not melting pots of genetic diversity. *Science* **300:** 1563–1565.

Phillips SJ, **Anderson RP**, **Schapire RE. 2006.** Maximum entropy modeling of species geographic distributions. *Ecological Modelling* **190:** 231–259.

Poldini L. 2009. *La diversità vegetale del Carso tra Trieste e Gorizia*. Trieste: Ed. Goliardiche.

Posada D. 2008. jModelTest: phylogenetic model averaging. *Molecular Biology and Evolution* **25:** 1253–1256.

R Core Team. **2016.** *R: a language and environment for statistical computing*. Vienna: R Foundation for Statistical Computing. Available at: http://www.R-project.org/ (date last accessed, 15 June 2019).

Rambaut A, **Drummond A. 2009.** *FigTree, version 1.3. 1*. Edinburgh: Institute of Evolutionary Biology.

Rambaut A, **Suchard MA**, **Xie D**, **Drummond AJ. 2015.** Tracer v1. 6 2014. Available at: http://beast.bio.ed.ac.uk/Tracer.

Riccieri A, **Maura M**, **Salvi D**, **Bologna MA**, **Mancini E. 2017.** Messinian Salinity Crisis and Quaternary glacial events shaped genetic diversification in Siculo-Maghrebian

blister beetles (Coleoptera: Meloidae). *Biological Journal of the Linnean Society* **122:** 455–468.

Riccieri A, **Mancini E**, **Salvi D**, **Bologna MA. 2020.** Phylogeny, systematic and biogeography of the hyperdiverse genus *Hycleus* Latreille, 1817 (Coleoptera: Meloidae). *Molecular Phylogenetics and Evolution* **144:** 106706.

Ronquist F, **Teslenko M**, **van der Mark P**, **Ayres DL**, **Darling A**, **Höhna S**, **Larget B**, **Liu L**, **Suchard MA**, **Huelsenbeck JP. 2012.** MrBayes 3.2: efficient Bayesian phylogenetic inference and model choice across a large model space. *Systematic Biology* **61:** 539–542.

Rozas J, **Ferrer-Mata A**, **Sánchez-DelBarrio JC**, **Guirao-Rico S**, **Librado P**, **Ramos-Onsins SE**, **Sánchez-Gracia A. 2017.** DnaSP 6: DNA sequence polymorphism analysis of large data sets. *Molecular Biology and Evolution* **34:** 3299–3302.

Sambrook J, **Fritsch EF**, **Maniatis T. 1989.** *Molecular cloning: a laboratory manual*. Cold Spring Harbor: Cold Spring Harbor Laboratory Press.

Salvi D, **Maura M**, **Pan Z**, **Bologna MA. 2019.** Phylogenetic systematics of *Mylabris* blister beetles (Coleoptera, Meloidae): a molecular assessment using species trees and total evidence. *Cladistics* **35:** 243–268

Salvi D, **Schembri PJ**, **Sciberras A**, **Harris DJ. 2014.** Evolutionary history of the Maltese wall lizard *Podarcis filfolensis*: insights on the 'Expansion–Contraction' model of Pleistocene biogeography. *Molecular Ecology* **23:** 1167–1187.

Santos AM, **Cabezas MP**, **Tavares AI**, **Xavier R**, **Branco M. 2015.** tcsBU: a tool to extend TCS network layout and visualization. *Bioinformatics* **32:** 627–628.

Schmitt T. 2007. Molecular biogeography of Europe: Pleistocene cycles and postglacial trends. *Frontiers in Zoology* **4:** 11.

Schmitt T. 2009. Biogeographical and evolutionary importance of the European high mountain systems. *Frontiers in Zoology* **6:** 9.

Schmitt T. 2017. Molecular biogeography of the high mountain systems of Europe: an overview. In: Catalan J, Ninot JM, Mercè Aniz M, eds. *High mountain conservation in a changing world*. Cham: Springer, 63–74.

Senczuk G, **Harris DJ**, **Castiglia R**, **Litsi Mizan V**, **Colangelo P**, **Canestrelli D**, **Salvi D. 2019.** Evolutionary and demographic correlates of Pleistocene coastline changes in the Sicilian wall lizard *Podarcis wagleriana*. *Journal of Biogeography* **46:** 224–237

Staden R, **Beal KF**, **Bonfield JK. 2000.** The Staden package. In: Misener S, Krawetz SA, eds. *Computer methods in molecular biology, bioinformatics methods and protocols*. Totowa: Humana Press Inc, 115–130.

Stamatakis A. 2006. RAxML-VI-HPC: maximum likelihood-based phylogenetic analyses with thousands of taxa and mixed models. *Bioinformatics* **22:** 2688–2690.

Stewart JR, **Lister AM**, **Barnes I**, **Dalén L. 2010.** Refugia revisited: individualistic responses of species in space and time. *Proceedings of the Royal Society B: Biological Sciences* **277:** 661–671.

Sumakov GG. 1915. Les espèces paléarctiques du genre *Mylabris* Fabr. (Coloptera, Meloidae). *Horae Societatis Entomologicae Rossicae* **42:** 1–71.

Taberlet P, **Fumagalli L**, **Wust-Saucy AG**, **Cossons JF. 1998.** Comparative phylogeography and postglacial colonization routes in Europe. *Molecular Ecology* **7:** 453–464.

Thuiller W, **Lafourcade B**, **Engler R**, **Araújo MB. 2009.** BIOMOD–a platform for ensemble forecasting of species distributions. *Ecography* **32:** 369–373.

Thuiller W, **Georges D**, **Engler R. 2016.** biomod2: ensemble platform for species distribution modeling. R package version 3.3–7. Available at: http://CRAN.R project.org/package=biomod2 (date last accessed 8 March 2019).

Todisco V, **Gratton P**, **Cesaroni D**, **Sbordoni V. 2010.** Phylogeography of *Parnassius apollo*: hints on taxonomy and conservation of a vulnerable glacial butterfly invader. *Biological Journal of the Linnean Society* **101:** 169–183.

Trizzino M, **Audisio P**, **Antonini G**, **De Biase A**, **Mancini E. 2009.** Comparative analysis of sequences and secondary structures of the rRNA internal transcribed spacer 2 (ITS2) in pollen beetles of the subfamily Meligethinae (Coleoptera, Nitidulidae): potential use of slippage-derived sequences in molecular systematics. *Molecular Phylogenetics and Evolution* **51:** 215–226.

Watanabe S, **Hajima T**, **Sudo K**, **Nagashima T**, **Takemura T**, **Okajima H**, **Nozawa T**, **Kawase H**, **Abe M**, **Yokohata T. 2011.** MIROC-ESM 2010: Model description and basic results of CMIP5-20c3m experiments. *Geoscientific Model Development* **4:** 845.

Wesche K, **Ambarl D**, **Kamp J**, **Torok P**, **Treiber J**, **Dengler J. 2016.** The Palaearctic steppe biome: a new synthesis. *Biodiversity and Conservation* **25:** 2197–2231.

Zhang L, **Liu S**, **Sun P**, **Wang T**, **Wang G**, **Zhang X**, **Wang L. 2015.** Consensus forecasting of species distributions: the effects of Niche model performance and Niche properties. *PLoS One* **10:** e0120056.

SUPPORTING INFORMATION

Additional Supporting Information may be found in the online version of this article at the publisher's web-site:

Figure S1. a, Bayesian tree based on *COI* sequences. Only supported values of Bayesian Posterior Probability are reported at each node (PP > 0.9). b, Bayesian tree based on ITS2 sequences. Only supported values of Bayesian Posterior Probability are reported at each node (PP > 0.9). c, Bayesian tree based on *CAD* sequences. Only supported values of Bayesian Posterior Probability are reported at each node (PP > 0.9). d, ML tree based on *COI* sequences. Only supported values of Bootstrap are reported at each node (BP > 70). e, ML tree based on ITS2

sequences. Only supported values of Bootstrap are reported at each node (BP > 70). f, ML tree based on *CAD* sequences. Only supported values of Bootstrap are reported at each node (BP > 70).

Table S1. Specimens used for phylogenetic analyses, with relative code, sampling locality and Genbank accession number for the three markers *CAD*, ITS2 and *COI*. Genbank accession numbers marked with * indicate sequences derived from Salvi *et al.* (2019) and Riccieri *et al.* (2020).

Table S2. Specimens used for phylogeographical analyses, with relative code, sampling locality and Genbank accession number for the two markers *CAD* and ITS2. Genbank accession numbers marked with * indicate sequences derived from Salvi *et al.* (2019) and Riccieri *et al.* (2020).